A Reliability-Oriented Design Method for Power Electronic Converters

Huai Wang, *IEEE Member,* Dao Zhou, *IEEE Student Member* and Frede Blaabjerg, *IEEE Fellow*
Center of Reliable Power Electronics (CORPE)
Department of Energy Technology, Aalborg University
Pontoppidanstraede 101, 9220 Aalborg, Demark
Email: hwa@et.aau.dk; zda@et.aau.dk; fbl@et.aau.dk

***Abstract*- Reliability is a crucial performance indicator of power electronic systems in terms of availability, mission accomplishment and life cycle cost. A paradigm shift in the research on reliability of power electronics is going on from simple handbook based calculations (e.g. models in MIL-HDBK-217F handbook) to the physics-of-failure approach and design for reliability process. A systematic design procedure consisting of various design tools is presented in this paper to design reliability into the power electronic converters since the early concept phase. The corresponding design procedures and reliability prediction models are provided. A case study on a 2.3 MW wind power converter is discussed with emphasis on the reliability critical component IGBT modules.**

I. INTRODUCTION

Advances in power electronics in the last four decades have enabled power converters exhibiting high efficiency and high power density. Recently, more and more efforts are devoted to reliability aspect due to the issues on availability, maintenance cost and safety in emerging applications (e.g., renewable energy conversion, electric vehicles and smart grid) [1]-[7]. Surveys are presented in [8]-[13] to analyze the failure examples, reliability prediction and on-line condition monitoring. It can be noted that the terms, such as bathtub curve, mean-time-to-failure (MTTF) and mean-time-between-failures (MTBF), are dominantly used to indicate the reliability of power electronic components and systems. Bathtub curve [14] describes three distinct periods of the operation of a device or system. While it is approximately consistent with some practical cases, the assumptions of "random" failures and constant hazard rate during the useful life period are misleading [14] and the true root causes of different failure modes are not identified. The fundamental assumptions of MTTF or MTBF are constant failure rate and no wear out. Therefore, their values have high degree of inaccuracy if wear out occurs within the estimated time. Moreover, MTTF represents the time when 63.2% of items would fail and varies with operation conditions and testing methods [15].

For reliability prediction, military handbook MIL-HDBK-217F [16] is widely used to predict the failure rate of electronic components [3]-[7]. However, temperature cycling, failure rate change with material, combined environments, supplier variations (e.g. technology and quality) are not considered. Moreover, as failure details are not collected and addressed, the handbook method could not give designers insight into the root cause of a failure and the inspiration for reliability enhancement. Physically, a failure rate of a component is the sum of the failure rates of various failure modes, which have different reliability prediction models corresponding to different failure mechanisms. Statistics is a necessary basis to deal with the effects of uncertainty and variability on reliability. However, as the variation is often a function of time and operating conditions, statistics itself is not sufficient to interpret the reliability data without judgment of the assumptions and non-statistical factors (e.g. modification of designs, new generation of components, etc.).

To perform reliability-oriented design, it is worthwhile to explore the major failure modes and failure mechanisms of all reliability-critical components. Fig. 1 and Fig. 2 show the failure distribution among power electronic components [10] and source of stresses that have significant impact on reliability [17].

To tackle the limitations of the dominant reliability research in the area of power electronics, this paper proposes a systematic method for reliability-oriented design for power electronic converters. A case study on a 2.3 MW wind power converter is presented with emphasis on the reliability critical IGBT modules.

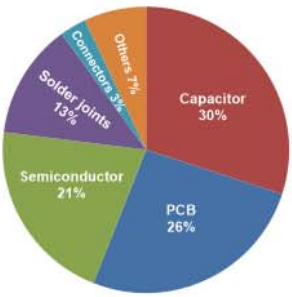

Figure 1. Failure root cause distribution for power electronic systems (Data source: [10]).

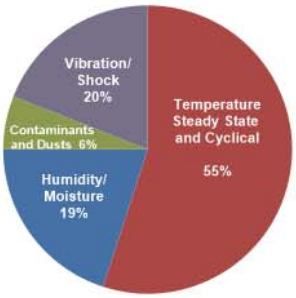

Figure 2. Source of stresses for electronic equipment (Data source: [17]).

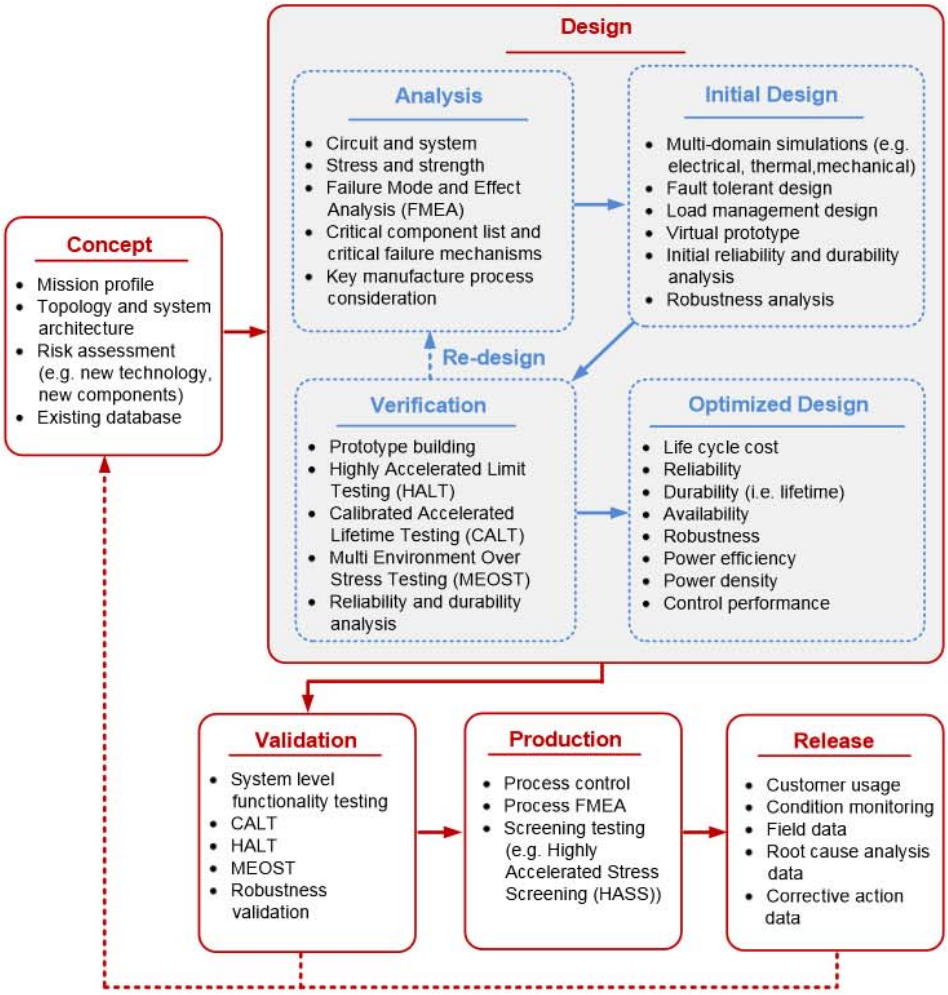

Figure 3. Proposed reliability-oriented design procedure for power electronic converters.

II. Proposed Reliability-Oriented Design Guideline

A systematic reliability-oriented design procedure specifically applicable to power electronic system is proposed as shown in Fig. 3. It can be noted that the procedure designs reliability into each development process (i.e. concept, design, validation, production and release) of power electronic products, especially in the design phase. Therefore, attention is given to the detailed procedures and various design tools applied in the design phase according to the initial design concept.

A. Concept Phase

In the initial concept phase, the conditions to which the power electronic converters are expected to be exposed (i.e. mission profile) are identified. Benchmarking of system architecture and circuit topology is conducted. Then, the potential new risks brought into the design are analyzed based on past experience and applied new type of devices and topologies. In the wind power application, the mission profile mainly depends on the wind speed profile. Therefore, it is necessary to analyze the feature of the wind profile based on record data of a specific location and time period. Fig. 4 gives an example of one year wind speed at records in Aalborg, Denmark.

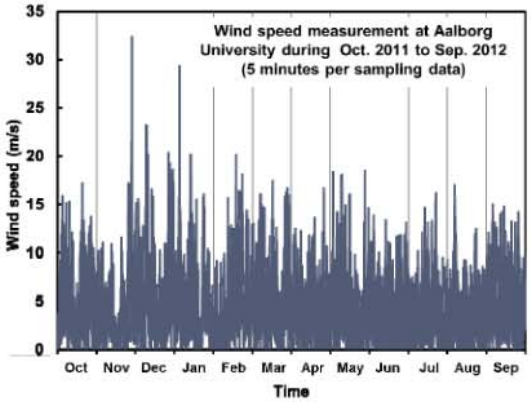

Figure 4. Example of one year wind speed profile.

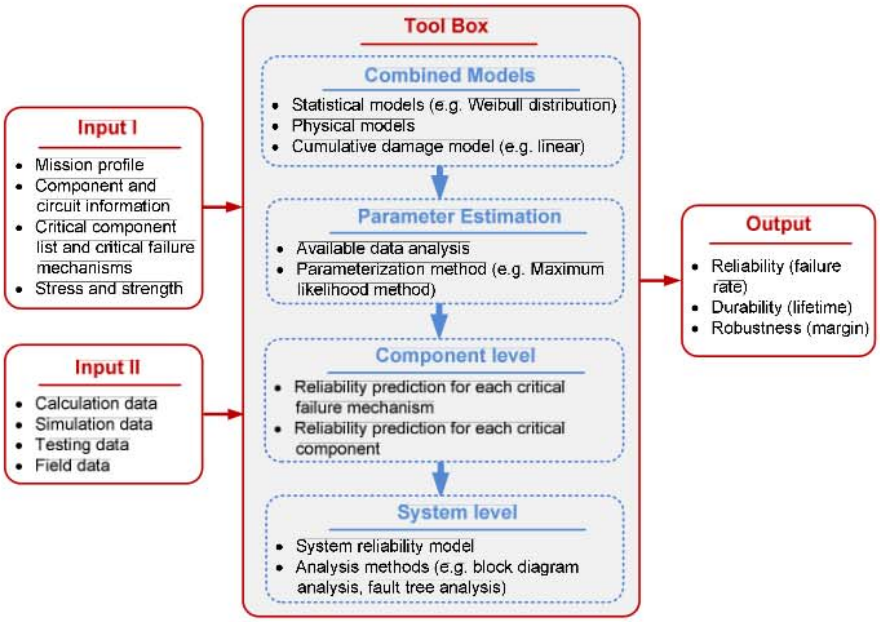

Figure 5. Proposed reliability prediction procedure for power electronic systems.

B. *Design Phase - Analysis*

The analysis covers the following four aspects: a) basic operation of the power electronic circuit and system; b) electrical and thermal stress analysis based on the system specifications and mission profile for preliminary selection of components to meet the stress-strength requirement; c) Failure Mode Effect and Analysis (FMEA) [18] to identify the failure mechanisms, failure mode (e.g. open circuit, short circuit, etc.), occurrence and severity level of the failure and likelihood of prior detection for each cause of failure and d) list of reliability critical components in the system and their associated failure mechanisms.

C. *Design Phase – Initial Design*

Multi-domain simulation, especially the electrical-thermal simulation is a very useful tool to virtually investigate the static and dynamic properties of the system to be designed as discussed in [21]-[22]. The link between the electrical domain and thermal domain is the power loss and thermal model of individual component. Finite Element Analysis (FEA) can be used for thermal study.

At this stage, an initial reliability prediction can be performed. Fig. 5 proposes a generic prediction procedure based on the PoF approach. The toolbox includes combined models and various sources of available data (e.g. manufacturer testing data, simulation data and field data, etc.) for the reliability prediction of individual components and then the whole system. Statistical models are well presented in [18] and will not be discussed here. Temperature and temperature cycling are the major stressors that affect the reliability performance as shown in Fig. 2, which will be more significant with the trend for high power density and high temperature power electronic systems.

III. Physical Models for the Impact of Temperature and Temperature Cycling

Temperature and temperature cycling are the major stressors that affect the reliability performance as shown in Fig. 2. Therefore, two physical models are derived to explore the impact of temperature and temperature cycling on reliability.

A. *Degradation Model for the Temperature Effect*

Fig. 6(a) illustrates the degradation of a material or device from initial stable state with free energy of E_1 to a degraded state with free energy of E_2. The driving force for this degradation is the free energy difference between E_1 and E_2, defined as ΔE. The heat induced by power losses in power electronic components provides the energy for the transformation from one state to another. The degradation rate is limited by the activation energy E_a. Define k_{foward}, $k_{reverse}$ and k_{net} as the degradation rate, recovery rate and net reaction rate, respectively. It can be derived that

$$k_{net} = k_{forward} - k_{reverse} = k_0 e^{-\left(\frac{E_a}{K_B T}\right)} \left[1 - e^{-\left(\frac{\Delta E}{K_B T}\right)}\right] \approx k_0 e^{-\left(\frac{E_a}{K_B T}\right)} \quad (1)$$

where $E_a = -K_B \left[\ln\left(k_{net}\right) / \left(1/T\right)\right]$, K_B is the Boltzmann's constant (8.62×10^{-5}eV/K), T is the temperature in Kelvin and k_0 is a material/device specific constant. It should be noted that the approximated result in (1) is the Arrhenius equation [23] which is widely used for reliability prediction.

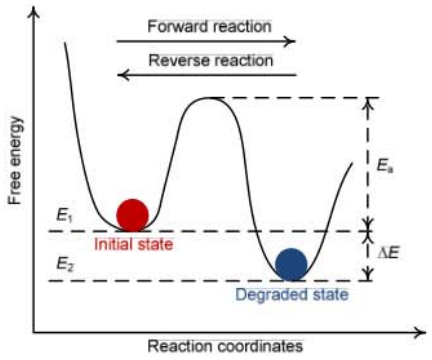

(a) Free energy description of material/device degradation.

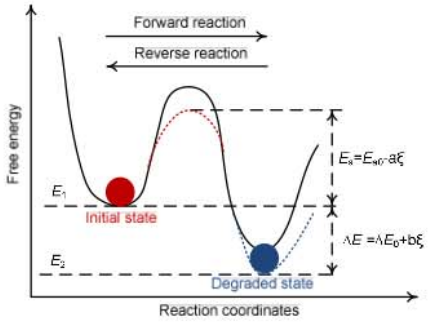

(b) The impact of additional stress on material/device degradation.

Figure 6. Material/device degradation from free energy perspective (adapted from [19]).

The value of the activation energy is dependent on the type of material and device, which can be obtained by the curve fitting of accelerated lifetime testing data under various temperatures.

When combined stresses are applied, the activation energy ΔE is dependent on additional applied stress □(e.g. electrical stress, mechanical stress, and chemical stress) as shown in Fig. 6(b). The parameters a and b are determined from stress-induced degradation testing data. a is temperature dependent and defined as $a = a_0 + a_1 K_B T$. It can be obtained that $k_{net} = k_0 \left(\frac{b}{K_B T}\right) x e^{-\left(\frac{E_{a0}}{K_B T}\right)}$ and $k_{net} = k_0 e^{a_1 x} e^{-\left(\frac{E_{a0} - a_0 x}{K_B T}\right)}$ under low □and high □ respectively. Therefore, a power law dependence for stress □is widely used to bridge the gap between low stress (k_{net} is linear with □) and high stress (k_{net} is exponential with □). That is

$$k_{net} = k_0 x^n e^{-\left(\frac{E_a}{K_B T}\right)} \tag{2}$$

B. *Lifetime Model for the Temperature Cycling Effect*

The thermal cycling is a response to the converter line and loading variations as well as periodically commutation of power switching devices. It will induce cyclic temperature stress on different layers of materials used for fabrication of power electronic components. According to the plastic and elastic behaviors analyzed in [19] and [24], it can be obtained that

$$N = k\left(\Delta T - \Delta T_0\right)^{-m} \tag{3}$$

where □and k are empirically-determined constants and N_f is the number of cycle to failure. ΔT is temperature cycle range and ΔT_0 is portion of ΔT that in the elastic strain range. If ΔT_0 is negligible compared to ΔT, it can be dropped out from the above equation and the equation turns to be the Coffin-Manson model as discussed in [2].

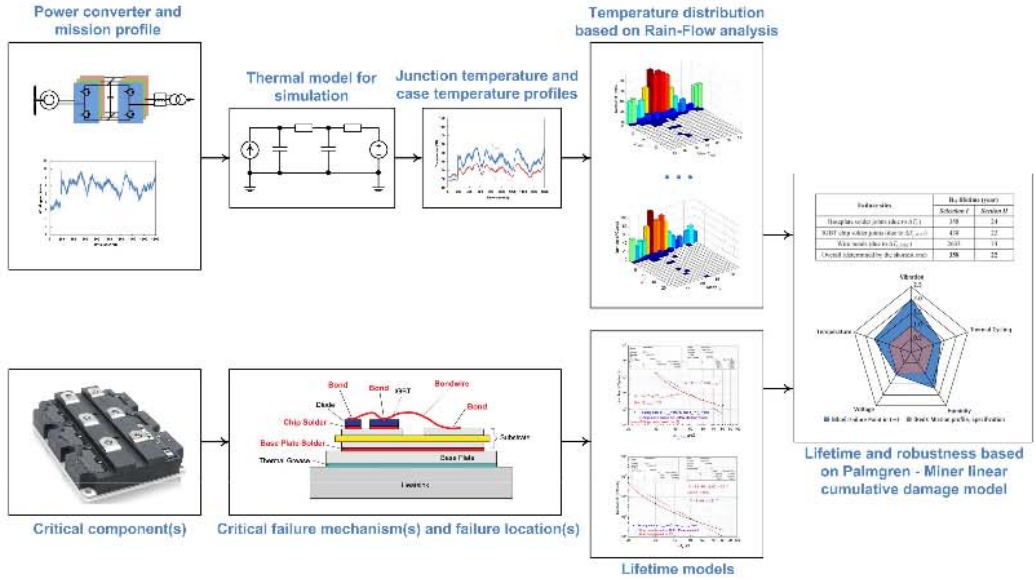

Figure 7. Lifetime prediction of the IGBT modules.

IV. Case Study on a 2.3 MW Wind Power Converter

The case study on a 2.3 MW wind power converter is performed as an example to demonstrate the proposed reliability-oriented design method. In this paper, the selection of the reliability critical component IGBT modules is focused. According to the general reliability prediction procedure shown in Fig. 5, a specific block diagram used for predicting the lifetime of IGBT modules is shown in Fig. 7. The following analysis follows the steps in Fig. 7.

A. Topology and Specification of the Converter

As shown in Fig. 8, the full-scale power converter in wind power configuration equipped with permanent magnet synchronous generator (PMSG) is considered as a promising technology for multi-MW wind turbine system. A two level back-to-back topology is applied for the application, which is a relatively simple structure with few components. Table I shows the specification of the power converter. For illustration purpose, IGBT modules in the grid-side converter are focused in this paper. Two kinds of selections of the IGBT modules are shown in Table I.

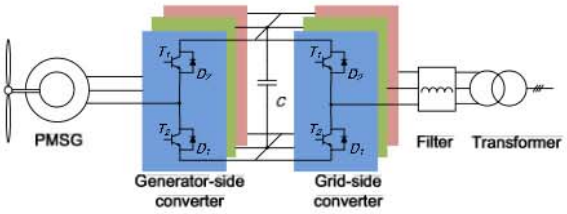

Figure 8. 2.3 MW Two level back-to-back wind power converter.

TABLE I. Converter Parameters for the Case Study.

Topology	2L-BTB as shown in Fig. 8
Rated output active power P_o	2.3 MW
DC bus voltage V_{dc}	1.1 kV DC
*Rated primary side voltage V_p	690V rms
Rated load current I_{load}	1.93 kA rms
Switching frequency f_c	1950 Hz
Filter inductance L_f	132 μH
IGBT *Selection I* (grid side)	1.6 kA/1.7 kV/125°C, two in parallel
IGBT *Selection II* (grid side)	2.4 kA /1.7 kV/150°C, single switch

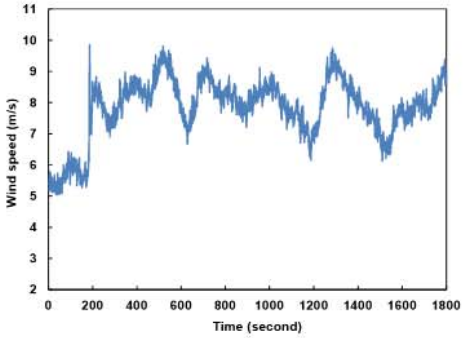

Figure 9. Wind speed profile for the case study.

B. The Studied Wind Speed Profile

For illustration purpose, a wind speed profile during a half hour shown in Fig. 9 is analyzed. It should be noted that for practical applications, the profiles are obtained by collecting wind speeds during a much longer time period.

C. Distribution of Temperature Profile and Temperature Cycling

Figs. 10 (a) and (b) show the case temperature and junction temperature of IGBT modules from *Selection I* and *Selection II*, respectively. It can be noted that IGBT modules with a lower current rating have higher amplitudes of ΔT_j and ΔT_c, thus, lower number of cycles to failure.

To perform the lifetime prediction, the analysis of the temperature cycling distribution is necessary. The Rainflow counting method [25] is applied to extract the temperature information as shown in Fig. 11. Figs. 11(a) and (b) show the case temperature and junction temperature cycling of the IGBT modules from *Selection I*. Figs.11(c) and (d) give those of the IGBT modules from *Section II*. The majority of the temperature cycling is of low amplitude (i.e. less than ΔT_0) which has negligible impact on the lifetime.

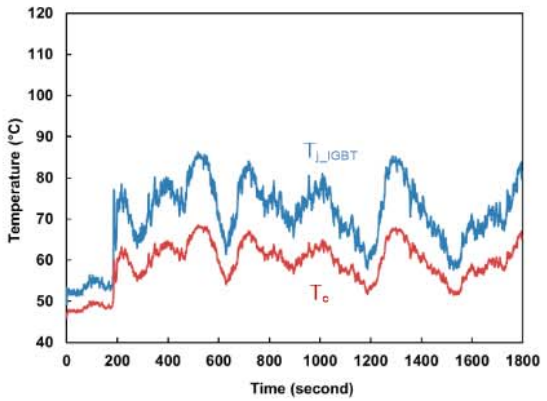

(a) The IGBT junction temperature and case temperature with *Selection I* of two 1.6 kA/1.7 kV IGBTs in parallel.

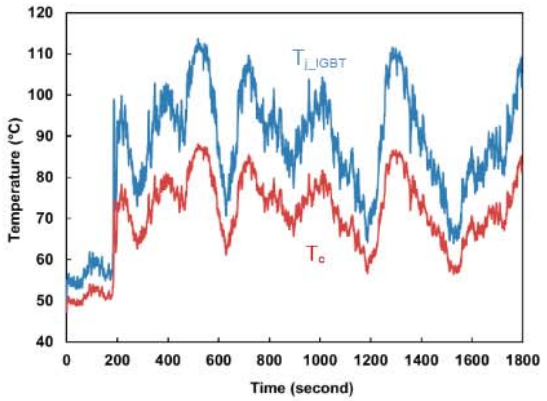

(b) The IGBT junction temperature and case temperature with *Selection II* of single 2.4 kA /1.7 kV IGBT.

Figure 10. Temperature profiles of the two kinds of selected IGBT modules.

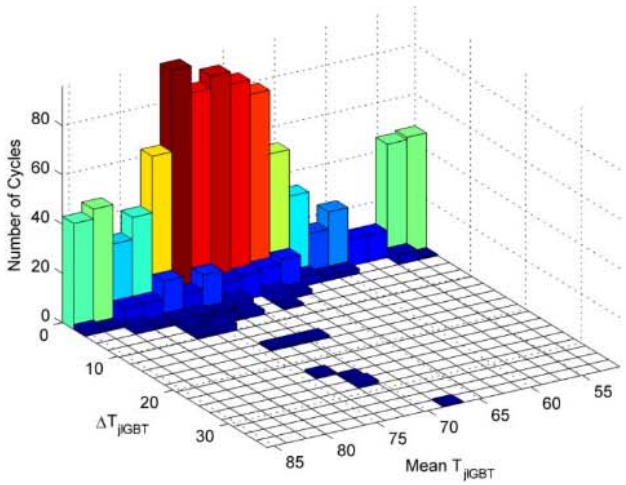

(a) Distribution of junction temperature cycling with *Selection I* of two 1.6 kA/1.7 kV IGBTs in parallel (Temperature unit: °C).

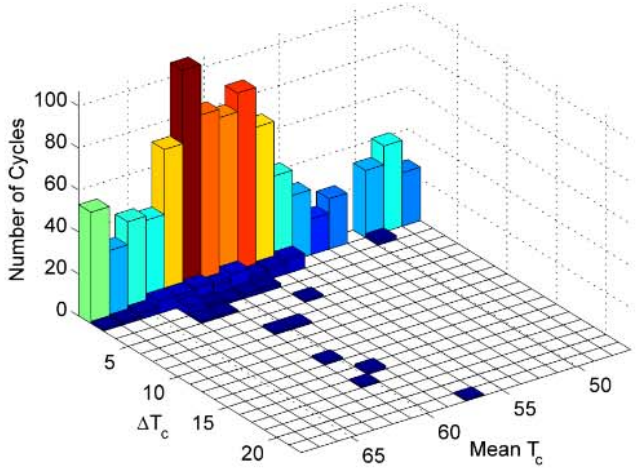

(b) Distribution of case temperature cycling with *Selection I* of two 1.6 kA/1.7 kV IGBTs in parallel (Temperature unit: °C).

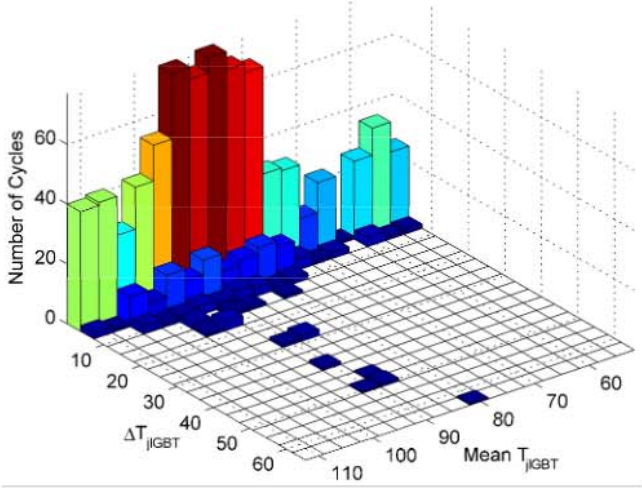

(c) Distribution of junction temperature cycling with *Selection II* of single 2.4 kA /1.7 kV IGBT (Temperature unit: °C).

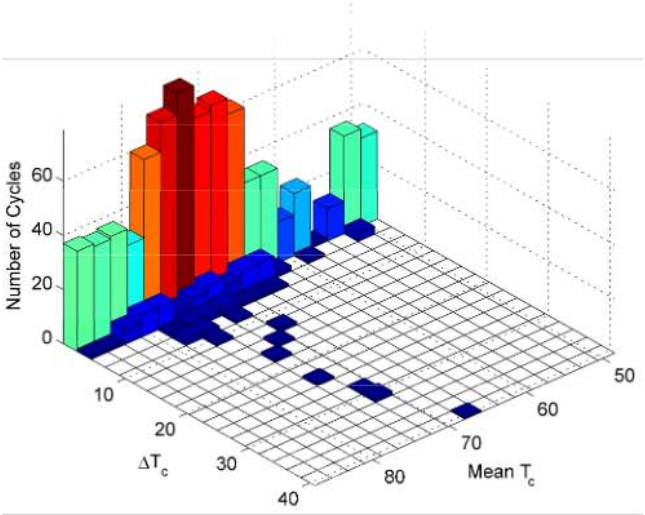

(d) Distribution of case temperature cycling with *Selection II* of single 2.4 kA /1.7 kV IGBT (Temperature unit: °C).

Figure 11. Rainflow counting of the temperature profiles of the IGBT modules.

D. IGBT Module Lifetime Prediction models

Thermal cycling is found to be one of the main drivers for the fatigue of IGBT modules. With a low cyclic temperature below $\Box T_0$, no damage occurs and the material is in the elastic region. When the stress is increased above $\Box T_0$, an irreversible deformation is induced and the material enters into the plastic region. The coefficients of thermal expansion for different materials in the IGBT modules are different, leading to stress formation in the packaging and continuous degradation with each cycle until the material fails.

As discussed in [26], there are three critical failure sites of IGBT modules: baseplate solder joints, chip solder joints, and the wire bonds. As the procedure shown in Fig. 5, a specific lifetime model is required for each failure mechanism. Therefore, the model shown in (3) is to be applied and the associated parameters for the three different failure sites are to be estimated respectively from testing data, which consider both the plastic and elastic behavior of the interface materials.

Moreover, as the amplitude and average temperature level of the thermal cycling are different when the wind is fluctuating, the Palmgren - Miner linear cumulative damage model [27] is applied in the form of

$$\sum_i \frac{n_i}{N_i} = 1 \tag{4}$$

where n_i is the number of applied temperature cycles at stress $\Box T_i$ and N_i is the number of cycles to failure at the same stress and for the same cycle type. Therefore, each type of $\Box T_i$ accounts for a portion of damage. Failure occurs when the sum of the left hand side of (4) reaches one.

E. Parameter Estimation of Lifetime Models

The manufacturer of the IGBT modules has performed a series of power cycling experiments as described in [26]. Based on the B_{10} lifetime testing data (which is the number of cycles when 10% of the total number of modules fail), the parameters of the derived model in (3) can be estimated as shown in Fig. 12.

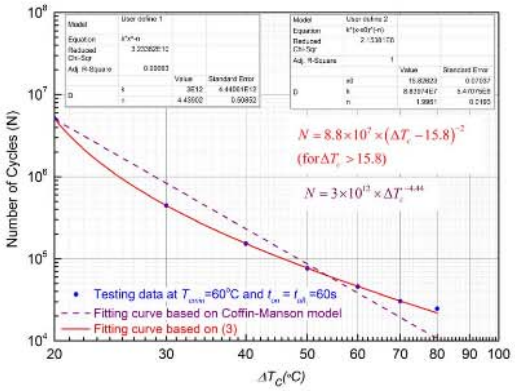

(a) Cycle to failure models for thermal cycling on baseplate solder joints for t_{cycle} = 120s and T_{cmin} = 60°C.

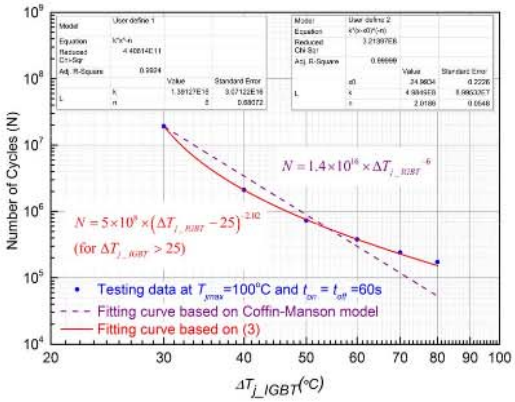

(b) Cycle to failure models for thermal cycling on chip solder joints for t_{cycle} = 120s and T_{jmax} = 100°C.

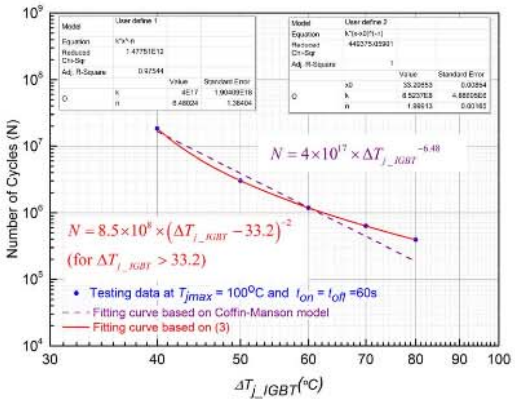

(c) Cycle to failure models for thermal cycling on wire bonds T_{jmax} = 100°C.

Figure 12. Parameter estimations based on the model derived in (3) and the Coffin-Mansion model (lifetime testing data source: [26]).

The lifetime testing data are also used to fit the widely used Coffin-Mansion model, in which the yield amplitude of the temperature cycling and therefore the elastic behavior are not taken into account. However, with large number of cycling ($> 10^4$) under low cyclic temperature stress, the absence of the elastic behavior may induce high level of inaccuracy. As shown in Fig. 12, the model in (3) fits the testing data better.

Moreover, the number of cycles to failure also depends on the average junction temperature T_j and average case temperature T_c. A scaling factor is provided by the manufacturer in [28] as

$$\text{Scaling factor} = 1.017^{\left(\Delta T_{level}^{1.16}\right)} \tag{5}$$

where ΔT_{level} is the difference between two maximum junction temperature levels or two minimum case temperature levels.

F. Lifetime Prediction Results

According to the calibrated models shown in Fig. 12, only the temperature cycling with $\Delta T_c > 15.8$°C, $\Delta T_{j\_IGBT} > 25$°C and $\Delta T_{j\_IGBT} > 33.2$°C is considered for the lifetime prediction of baseplate solder joints, IGBT chip solder joints and wire bonds, respectively. The impact of the ones with lower amplitude is sufficiently to be neglected. For illustration purpose, the wind profile is assumed to repeat as that in the analyzed half hour and the wind turbine operates 24 hours per day and 365 days per year. According to the models based on (3) in Fig. 12 and the ones shown in (4) and (5), the lifetime of the two selected IGBT modules is predicted and the results are given in Table II.

It should be noted that the purpose of the case study on the IGBT modules is to demonstrate the procedure to perform reliability prediction based on mission profile and PoF approach with differentiation of various failure sites. For practical considerations, wind speed profile during long time period at specific location needs to be collected and analyzed. Therefore, wind profile as shown in Fig. 4 could be useful for future research. Moreover, other failure mechanisms in IGBT modules may induce additional failures and should also be considered in the lifetime estimation. The failure rates of other reliability critical components are also required to be taken into account for the system level prediction of failure rate and lifetime.

TABLE II. LIFETIME PREDICTION RESULTS.

Failure sites	B_{10} lifetime (year)	
	Selection I	*Section II*
Baseplate solder joints (due to ΔT_c)	358	24
IGBT chip solder joints (due to ΔT_{j_IGBT})	438	22
Wire bonds (due to ΔT_{j_IGBT})	2633	74
Overall (determined by the shortest one)	**358**	**22**

CONCLUSIONS

A reliability-oriented design method is proposed for achieving more reliable power electronic converters. Lifetime models revealing the impact of temperature and temperature cycling are derived. A case study on a 2.3 MW wind power converter has been demonstrated. The detailed procedure for lifetime prediction of the applied IGBT modules is discussed. It is based on analysis on the mission profile, failure mechanism, thermal profile and the parameter estimation of associated lifetime models.

REFERENCES

[1] E. Koutroulis and F. Blaabjerg, "Design optimization of transformer-less grid-connected PV inverters including reliability," *IEEE Transactions on Power Electronics*, vol. 28, no. 1, pp. 325-335, Jan. 2013.

[2] C. Busca, R. Teodorescu, F. Blaabjerg, S. Munk-Nielsen, L. Helle, T. Abeyasekera and P. Rodriguez, "An overview of the reliability prediction related aspects of high power IGBTs in wind power applications, " *Journal of Microelectronics Reliability*, vol. 51, no. 9-11, pp. 1903-1907, 2011.

[3] S. V. Dhople, A. Davoudi, A. D. Dominguez-Garci and P. L. Chapman, "A unified approach to reliability assessment of multiphase DC-DC converters in photovoltaic energy conversion systems," *IEEE Trans. Power Electron.*, vol. 27, no. 2, pp. 739- 751, Feb. 2012.

[4] R. Burgos, C. Gang, F. Wang, D. Boroyevich, W. G. Odendaal and J. D. V. Wyk, "Reliability-oriented design of three-phase power converters for aircraft applications, " *IEEE Trans. Aerosp. Electron. Syst.,* vol. 48, no. 2, pp. 1249-1263, Apr. 2012.

[5] A. Ristow, M. Begovic, A. Pregelj and A. Rohatgi, "Development of a methodology for improving photovoltaic inverter reliability, " *IEEE Trans. Ind. Appl.*, vol. 55, no. 7, pp. 2581-2592, Jul., 2008.

[6] C. Rodriguez and G. A. J. Amaratunga, "Long-lifetime power inverter for photovoltaic AC modules, " *IEEE Trans. Ind. Electron.*, vol. 55, no. 7, pp. 2593-2601, Jul. 2008.

[7] F. Chan and H. Calleja, "Design strategy to optimize the reliability of grid-connected PV systems, " *IEEE Trans. Ind. Electron.,* vol. 56, no. 11, pp. 4465-4472, Nov., 2009.

[8] M. Boettcher and F. W. Fuchs, "Power electronic converters in wind energy systems -considerations of reliability and strategies for increasing availability," *in Proc. of European Conf. on Power Electron. and Appl.*, 2011.

[9] R. Johan and B. L. Margareta, "Survey of failures in wind power systems with focus on Swedish wind power plants during 1997-2005," *IEEE Trans. Energy Convers.*, vol. 22, no. 1, pp. 167-173, Mar. 2007.

[10] E. Wolfgang, "Examples for failures in power electronics systems," presented at *ECPE Tutorial on Reliability of Power Electronic Systems*, Nuremberg, Germany, Apr. 2007.

[11] S. Yang, A. T. Bryant, P. A. Mawby, D. Xiang, L. Ran, and P. Tavner, "An industry-based survey of reliability in power electronic converters," *IEEE Trans. Ind. Appl.*, vol. 47, no. 3, pp. 1441- 1451, May/Jun.,2011.

[12] Y. Song and B. Wang, "Survey on reliability of power electronic systems," *IEEE Transactions on Power Electronics*, vol. 28, no. 1, pp. 591-604, Jan. 2013.

[13] S. Yang, D. Xiang, A. Bryant, P. Mawby, L. Ran and P. Tavner, "Condition monitoring for device reliability in power electronic converters: a review," *IEEE Trans. Power Electron.*, vol. 25, no. 11, pp. 2734-2752, Nov., 2010.

[14] G. A. Klutke, Peter C. Kiessler, and M. A. Wortman, "A critical look at the Bathtub curve," *IEEE Trans. Rel.*, vol. 52, no. 1, pp. 125-129, Mar., 2003.

[15] M. Krasich, "How to estimate and use MTTF/MTBF would the real MTBF please stand up?" *in Proc. of IEEE Annual Rel. and Maintain. Symp.*, 2009.

[16] Military Handbook: *Reliability prediction of electronic equipment*, MIL-HDBK-217F, Dec. 2, 1991.

[17] ZVEL, *Handbook for robustness validation of automotive electrical/electronic modules*, Jun. 2008

[18] P. O'Connor, A. Kleyner, *Practical reliability engineering*, the 5th edition, John Wiley & Sons, 2012.

[19] J. W. McPherson, *Reliability physics and engineering: time-to-failure modeling*, Springer, 2010.

[20] A. Wintrich, U. Nicolai, W. Tursky and T. Reimann, *Application manual power semiconductors*, SEMIKRON International, pp. 122, 2011.

[21] J. Biela, J. W. Kolar, A. Stupar, U. Drofenik, and A. Muesing, "Towards virtual prototyping and comprehensive multi-objective optimization in power electronics," *in Proc. of PCIM* 2010, Nuremberg, pp. 1-23, 2010.

[22] D. Bin, J. L. Hudgins, E. Santi, A. T. Bryant, P. R. Palmer, and H. A. Mantooth, "Transient electrothermal simulation of power semiconductor devices," *IEEE Transactions on Power Electronics*, vol. 25, no. 1, pp. 237-248, Jan. 2010.

[23] M. S. Cooper, "Investigation of Arrhenius acceleration factor for integrated circuit early life failure region with several failure mechanisms," *IEEE Transactions on Components and Packaging Technologies*, vol. 28, no. 3, pp. 561-563, Sep. 2005.

[24] Huai Wang, Ke Ma, and Frede Blaabjerg, "Design for Reliability of Power Electronic Systems," *in Proc. of IEEE Industrial Electronics Society Annual Conference*, pp. 33-44, 2012.

[25] ASTM International, *E1049-85 (2005) Standard practices for cycle counting in fatigue analysis*, 2005.

[26] ABB Application Note, *Load-cycling capability of HiPak™ IGBT modules*, 2012.

[27] Miner, M. A., "Cumulative damage in fatigue," *Journal of Applied Mechanics*, no. 12, A159-A164, 1945.

[28] ABB Application Note, *Load-cycling capability of HiPaks*, 2004.